Chemical Engineering Journal 165 (2010) 225–233

Contents lists available at ScienceDirect

Chemical Engineering Journal

journal homepage: www.elsevier.com/locate/cej

Photocatalytic inactivation of *Escherischia coli* and *Pichia pastoris* with combustion synthesized titanium dioxide

Sharad Sontakke, Jayant Modak, Giridhar Madras*

Department of Chemical Engineering, Indian Institute of Science, Bangalore 560012, Karnataka, India

ARTICLE INFO

Article history:
Received 28 July 2010
Received in revised form
15 September 2010
Accepted 16 September 2010

Keywords:
Photocatalysis
Combustion synthesis
TiO_2
Ag/TiO_2
E. coli
Pichia pastoris

ABSTRACT

The photocatalytic inactivation of *Escherischia coli* and *Pichia Pastoris* was studied with combustion synthesized titanium dioxide photocatalysts. Three different combustion synthesized (CS) catalysts were used viz., CS–TiO_2, 1% Ag substituted in TiO_2 and 1% Ag impregnated in TiO_2. All the combustion synthesized catalysts showed higher activity as compared to the activity observed with commercial Degussa P-25 TiO_2. The effect of various parameters like catalyst loading, different catalysts and initial cell concentration was studied. At the optimum loading, 1% Ag impregnated TiO_2 showed the maximum efficiency and complete inactivation of both the microorganisms was observed within an hour of irradiation. The morphology of inactivated cells was studied by inverted microscope and SEM. From the images obtained, it was hypothesized that damage to the cell wall was the main cause of cell inactivation. The initial cell concentration had a prominent effect on the inactivation. At a low initial cell concentration, the complete inactivation of *E. coli* and *P. pastoris* was observed within 10 and 20 min, respectively. This shows that *P. pastoris* has a stronger resistance towards photocatalytic inactivation than *E. coli*. The inactivation reactions were modeled with power law kinetics. The order of reaction in case of *E. coli* and *P. pastoris* were determined as 1.20 and 1.08, respectively.

1. Introduction

Photocatalytic inactivation of microorganisms, using semiconductor catalysts, has received considerable attention in the past two decades. Matsunaga et al. [1] were the first to report the use of Pt/TiO_2 semiconductor powder for photochemical sterilization of microorganisms. Since then, photocatalysis has been shown as an efficient process for the removal of a wide variety of microorganisms including pathogenic bacteria, fungi and viruses [2]. Many photocatalytic disinfection studies have been carried out to determine the effect of various parameters like light intensity [3,4], catalyst concentration [3–5], temperature [6], culture media [7], initial concentration of microorganism [4,6], pH [7], etc. on the inactivation of microorganisms to understand the underlying mechanism.

Various hypotheses regarding the mechanism of microorganism inactivation have been proposed. Matsunaga et al. [1] proposed that the direct photochemical oxidation of intracellular coenzyme A (CoA) was the main cause for inhibition in respiration of cells that led to cell death. Maness et al. [8] suggested that TiO_2 photocatalysis promotes the peroxidation of polyunsaturated phospholipids and induces major disordering of cell membrane in *Escherischia coli*. Sunada et al. [9] have suggested, the cell wall of *E. coli* undergoes disruption by disordering outer membranes and the reactive species (e.g., $HO^\bullet$, $HO_2^\bullet$, H_2O_2) penetrates the cytoplasmic membrane, leading to cell death. It is generally assumed that the reactive oxygen species (ROS) like H_2O_2, $O_2^\bullet$, etc. as well as hydroxyl radical ($HO^\bullet$), which are generated on the surface of UV-illuminated TiO_2, plays the major role for the inactivation of microorganisms [4,5,9]. Most of the inactivation studies are based on *E. coli* or other bacterial species. However, the inactivation kinetics for yeast has not been investigated.

TiO_2 is the most widely used catalyst in photocatalytic studies because of its high photocatalytic activity, non-toxicity and wide availability. Most of the degradation studies have used commercially available TiO_2, Degussa P-25 (DP-25) directly or in its modified form [4–7]. This commercial catalyst consists of 80% anatase and 20% rutile phase. However, anatase phase TiO_2 has been reported to possess higher photocatalytic activity than the rutile phase [10]. This catalyst has shown to remove a wide variety of organic and inorganic contaminants [11,12]. There are several methods for the synthesis of anatase phase TiO_2 [13–15]. Solution combustion synthesis [16] is a single step process to produce pure anatase phase TiO_2 and the catalyst produced by this method has been shown to be superior to the commercially available DP-

* Corresponding author. Tel.: +91 80 22932321; fax: +91 80 23601310.
E-mail addresses: giridhar@chemeng.iisc.ernet.in, giridharmadras@gmail.com (G. Madras).

1385-8947/$ – see front matter © 2010 Elsevier B.V. All rights reserved.
doi:10.1016/j.cej.2010.09.021

25 catalyst for the degradation of various chemical contaminants [17–19].

The important step in photocatalysis is generation of electron–hole pair. However, high rates of electron–hole recombination on catalyst surface results in low efficiency of the process [12]. To avoid this recombination, several studies have reported the deposition or impregnation of a transition metal on the TiO_2 surface [20–22]. The transition metal ions act as electron scavenger, which leads to an increase in the rate of formation of $HO^{\bullet}$ radicals [18]. The effect of metal ion can also be studied by either doping or substituting the metal into TiO_2. For the microorganism inactivation studies, silver is widely used [21,22] because of its well-known antimicrobial property.

E. coli is a common microorganism, usually found in the lower intestine of human and other warm-blooded organisms. It is also widely used as an indicator of fecal contamination. Most of the coliform strains are harmless, but some of the strains can cause serious food poisoning in humans. *E. coli* is, therefore, a popular model bacterium for the study of photocatalytic inactivation. Fungal strains such as *Aspergillus flavus* are reported to cause harmful diseases in human [23]. Photocatalytic inactivation of various fungal species has been reported [1,20,24–26]. Among fungi, *Saccharomyces cerevisiae* (*S. cerevisiae*) is well studied as a model microorganism because of its wide availability [1,20]. Some authors have also reported the antibacterial activity of an activated carbon fibre supporting silver against *E. coli*, *S. cerevisiae* and *Pichia pastoris* (*P. pastoris*) [27]. The advantage of using *P. pastoris*, as a model microorganism, is its similarity to *S. cerevisiae*. It can also be grown to higher densities than *S. cerevisiae* in a simple media [28].

There is no report till date for the photocatalytic inactivation of microorganisms with combustion synthesized catalysts. No studies on the photocatalytic inactivation of *P. pastoris* by any catalyst are available. In the present study, we have investigated the effect of unsubstituted combustion synthesized TiO_2 (CS–TiO_2), combustion synthesized 1% Ag substituted TiO_2 (Ag/TiO_2 (Sub)) and 1% Ag impregnated TiO_2 (Ag/TiO_2 (Imp)) on the photocatalytic inactivation of *E. coli* and *P. pastoris*. The effect of catalyst loading, catalysts and initial concentration on the inactivation of these microorganisms was studied. The microorganism cell morphology during the course of inactivation was studied by inverted microscope and SEM images. The kinetics of inactivation was also investigated and power-law kinetics was used to determine the rate constants and the order of the inactivation reaction.

2. Experimental

2.1. Materials and methods

2.1.1. Photocatalysts: preparation and characterization

The photocatalysts used in present study were CS–TiO_2, Ag/TiO_2 (Sub), Ag/TiO_2 (Imp), and DP-25. Al_2O_3 and Ag/Al_2O_3 (Imp) and were also used in order to check the effect of silver impregnation on the inactivation. CS–TiO_2 was prepared by using precursor titanyl nitrate ($TiO(NO_3)_2$) and fuel, glycine ($H_2N–CH_2–COOH$) (Merck, India). The controlled hydrolysis of titanium isopropoxide ($Ti(i\text{-}OPr)_4$) gives titanyl hydroxide ($TiO(OH)_2$), which on further reaction with nitric acid gives titanyl nitrate. Further details of the preparation have been described elsewhere [19]. Ag/TiO_2 (Sub) was synthesized from the combustion mixture containing $TiO(NO_3)_2$, $AgNO_3$ and glycine in the molar ratio 0.99:0.01:1.1. Ag/TiO_2 (Imp) was prepared by adding calculated amount of $AgNO_3$ drop wise to an aqueous suspension (100 mL) of CS–TiO_2 in presence of reducing agent, hydrazine hydrate (Ranbaxy, India), under magnetic stirring at room temperature. To recover the catalyst from aqueous suspension, it was dried at 150 °C for 24 h [29]. Similar procedure was followed for the synthesis of Ag/Al_2O_3 (Imp) catalyst.

DP-25 (BET surface area 50 m^2/g) was received as a gift from Degussa Inc. and was used for the comparison. Al_2O_3 (0.6–1.2 mm, as received) was obtained from Oxide India Pvt., Ltd., Durgapur, India. It was grinded (crystallite size: 20 ± 5 nm) and then used.

The catalysts were characterized by X-ray diffraction (XRD), transmission electron microscopy (TEM), Scanning electron microscope (SEM), Brunauer–Emmett–Teller (BET) surface area, thermogravimetric analysis (TGA), UV–vis spectroscopy and photoluminescence spectra. XRD patterns were recorded on Philips X'pert PANalytical diffractometer using CuKα radiation in the 2θ range from 10° to 80° at a scanning rate of 2°/min. TEM of catalyst powders was carried out using a JEOL JEM-2000 FX II transmission electron microscope. SEM was carried out by using Carl Zeiss Ultra 55 scanning electron microscope. The BET surface area was determined using Smart Sorb 92/93 apparatus. TGA was studied in the temperature range of 30–700 °C using Perkin-Elmer Pyris Diamond apparatus. UV–vis absorption spectra of catalysts were obtained using a UV–vis spectrophotometer (Perkin-Elmer Lambda 35) between 300 nm and 800 nm. Photoluminescence spectra of catalysts were recorded in Perkin Elmer LS 55 luminescence spectrometer at an excitation wavelength of 285 nm.

2.1.2. Microorganisms and growth media

E. coli K-12 MG 1655, a bacterial strain, and *P. pastoris* X-33, a yeast strain, were used as model microorganisms in this study. *E. coli* was obtained from the culture collections locally and was grown aerobically in Luria-Bertani (LB) broth (HiMedia, India) at 37 °C. *P. pastoris* was obtained from Invitrogen, USA and was grown aerobically at 30 °C in Yeast extract-Peptone-Dextrose (YPD) (HiMedia, India) as per Invitrogen protocol. Solid medium of agar plates was prepared using respective media and 2% agar powder (HiMedia, India) and was used in the plate count method for the analysis of inactivated samples.

2.1.3. Photochemical reactor

The schematic diagram of the photochemical reactor used in this study is shown in Fig. SI 1 (see supplementary information). It consisted of two parts: the jacketed quartz tube and a pyrex glass container. The jacketed quartz tube has the following dimensions: 3.4 cm i.d., 4 cm o.d., and 21 cm length. A high pressure mercury vapor lamp of 125 W (315–400 nm, UV-A) was placed inside the quartz tube. The tube was placed in a glass container and the microorganism-catalyst solution was taken in the glass container. The light source radiated predominantly at a wavelength of 365 nm corresponding to the energy of 3.4 eV. Further details of the reactor are presented elsewhere [19].

2.2. Experimental procedure

All the necessary glassware, centrifuge tubes, micropipette tips and deionized water (Millipore Milli-Q, 18 MΩ-cm) used for the experiments were autoclaved at 121 °C for 4 h. Cultures were prepared from freshly prepared inoculums in 100 mL of respective growth media in shaking incubator (Orbitek, India) at 200 rpm. The culture was centrifuged at 3500 rpm for 15 min and washed twice with sterile deionized water. After centrifuging and washing, the pallets were resuspended in 100 mL sterile deionized water. This suspension was then used for the inactivation experiment both in the presence or absence of catalyst. Lower initial cell concentrations were obtained by diluting the culture. The catalyst-microorganism suspension was stirred uniformly using a magnetic stirrer during the course of reaction. Water was circulated through the annulus of the jacketed quartz tube to avoid the excess heating due to dissipative loss of the UV energy during the reaction.

E. coli inactivation experiments were carried out with two different reactor configurations. In the first set of experiments the quartz tube and the lamp position was at a distance 20 cm away the solution and in the next set of experiments, the lamp was kept close to the solution by touching the solution. The photon flux and light intensity were measured by o-nitrobenzaldehyde actinometry [30]. The photon flux for the first and second configuration was calculated to be 2 W/m^2 and 64 W/m^2, respectively, with the corresponding light intensity of 1.34×10^{-7} Einstein/(L s) and 4×10^{-6} Einstein/(L s), respectively.

The inactivated samples were analyzed by standard plate count method i.e. by counting the colonies on each agar plate and then recording them. For analysis, 100 μL of suspension was collected after regular intervals. The samples were diluted, in sterile deionized water, such that the final count was not more than 200 cfu/mL (cfu = colony forming unit), and 100 μL of the diluted sample was spread on sterile agar plates. The experiments were carried out at least twice to check their reproducibility and the error was less than 5% in plate count.

The morphology of the cells was studied using an inverted microscope (Leica DM-IRB) and cells were photographed using Cohu high performance CCD camera. FEI Quanta ESEM was used for the SEM images. The samples for SEM analysis were fixed in 2% glutaraldehyde for 4 h at room temperature and then rinsed twice with distilled water. The samples were then treated with 1% osmium tetroxide for 1 h and finally dehydrated in an ascending series of ethanol solutions. The sample loaded silicon wafers were glued on a stub, which was then coated with 20 nm of gold using sputter coater.

3. Results and discussion

3.1. Catalyst characterization

The crystallite sizes determined from XRD pattern using Sherrer formula are 9 ± 2 nm for CS–TiO_2, 9 ± 2 nm for Ag/TiO_2 (Sub) and 10 ± 2 nm for Ag/TiO_2 (Imp) (Fig. SI 2 (see supplementary information)).

The XRD pattern of Ag/TiO_2 (Sub) shows all the characteristic peaks of anatase TiO_2, without any impurity peak corresponding to Ag or to rutile phase. This shows that Ag is substituted for Ti in the lattice. The impregnation of 1% Ag on CS–TiO_2 results in the formation of Bragg peaks at 38.2°, 44.3°, 64.5° and 77.5° corresponding to (1 1 1), (2 0 0), (2 2 0) and (3 1 1) plane reflection. These results show that Ag^+ is reduced to Ag^0, and is well dispersed on the surfaces of CS–TiO_2 [29].

Full profile Rietveld refinement of 1% Ag/TiO_2 (Sub) was carried out using GSAS. Initially, the cell parameters of TiO_2, $a = 3.7865$ Å and $c = 9.5091$ Å, were taken. Full occupancy was assigned to Ti, O and Ag, and the isotropic thermal parameters, unit cell and background parameters were refined. The cell parameters of 1% Ag/TiO_2 (Sub) were found to be: $a = 3.785(1)$ Å and $c = 9.527(1)$ Å, with a cell volume of 136.488(1) Å^3 and a cell density of 3.917 g cm^{-3}. As the radius of Ag^+ ion (ca. 1.26 Å) is larger than that of Ti^{4+} ion (ca. 0.68 Å), the increase in cell parameter indicates the substitution of Ag in the TiO_2 lattice [29].

The particle size determined by TEM (Figs. SI 3(a), SI 3(b) (see supplementary information)) and SEM (Fig. SI 4 (see supplementary information)) is consistent with the crystallite size determined by XRD. The ring type electron diffraction pattern of Ag/TiO_2 (Sub) and Ag/TiO_2 (Imp) are shown in Fig. SI 3(c) (see supplementary information). The presence of extra ring in the electron diffraction pattern of Ag/TiO_2 (Imp) suggests the deposition of Ag on the CS–TiO_2 surface. The dark field TEM images of Ag/TiO_2 (Imp) shows, and thereby confirms, the presence of Ag clusters on the surface of CS–TiO_2 (Fig. SI 3(d) (see supplementary information)). SEM images of different combustion synthesized catalyst are shown in Fig. SI 4 and are in good agreement with the catalyst sizes calculated with XRD and TEM. The BET surface areas measured for CS–TiO_2, Ag/TiO_2 (Sub), Ag/TiO_2 (Imp), are 150, 113 and 125 m^2/g respectively. The total weight loss calculated from TGA studies is 24.0% for CS–TiO_2, 14.2% for Ag/TiO_2 (Sub) and 18.6% for Ag/TiO2 (Imp) (Fig. SI 5 (see supplementary information)).

Three regions of weight loss were observed: (1) from room temperature to 150 °C, which is caused by the loss of physically adsorbed water, (2) 150–450 °C and is due to the removal of strongly bound water or surface hydroxyl groups from the catalyst and (3) from 450 to 680 °C. Thermal desorption studies from room temperature to 450 °C in a vacuum was carried out, and the results indicate that the primary species to leave the surface of TiO_2 is water. Thus, the weight loss can be attributed to hydroxyl groups [17] and this was further confirmed by FTIR [17]. The band gap energies (Eg) obtained from UV–vis spectrophotometry are 3.02 eV, 3.02 eV and 3.06 eV CS–TiO_2, Ag/TiO_2 (Sub) and for Ag/TiO_2 (Imp), respectively (Fig. SI 6 (see supplementary information)). The fluorescence spectra (Fig. SI 7 (see supplementary information)) of Ag/TiO_2 (Sub) and Ag/TiO_2 (Imp) exhibit emission peaks at 425 nm and 489 nm. The emissions at 425 and 489 nm can be attributed to the free excitation, and the transition from defect sites like oxygen vacancy to the Ti(3d) state, respectively [17]. Further details of characterization of Ag/TiO_2 can be found elsewhere [29].

3.2. Inactivation of microorganisms

3.2.1. Effect of catalyst loading

Fig. 1(a) shows the results of photocatalytic inactivation of *E. coli*, exposed to different loadings of CS–TiO_2 catalyst ranging from 0.1 to 0.5 g/L. The experiments were carried out with a light intensity of 2 W/m^2. The initial cell concentration was approximately 10^8 cfu/mL. The control experiment (without any catalyst) is indicated as "photolysis" and the experiment without UV (catalyst alone) is indicated as "dark". With photolysis, a 3.7-log reduction in plate count was observed within 60 min of irradiation time. On the other hand, there was no reduction in the dark experiment. When the catalyst loading was 0.1 g/L, a slight increase in the inactivation rate was observed. Increasing the catalyst concentration from 0.1 to 0.25 g/L increased the inactivation rate rapidly and a maximum 7-log reduction in the plate count was observed with the catalyst load. A further increase in the catalyst loading, from 0.25 g/L to 0.3 g/L, decreased the rate of inactivation and at high concentration of 0.5 g/L, the inactivation rate decreased even further. This indicates 0.25 g/L is the optimum catalyst loading for this system.

The reaction rate increases with catalyst loading up to a certain loading. At higher loadings, the effective light intensity is diminished because of the increased solution opacity. This results in lower activity and this observation is consistent with earlier reports [4,19]. When the photocatalyst concentration was 0.1 g/L, the low amount of catalyst was insufficient to inactivate large mass of cells and thus the inactivation was similar to that observed with photolysis. The increase in the inactivation rate with the increase in catalyst loading till 0.25 g/L shows the possibility of presence of more ROS, which is sufficient to damage the present cell mass. The optimum catalyst loading of 0.25 g/L could be attributed to the presence of maximum amount of ROS, by complete absorption of irradiated UV light, and the maximum interaction of those with the cell mass. When catalyst loading was increased beyond 0.25 g/L, more number of ROS could be expected. However, the high amounts of catalyst result in turbidity and thus actually block the radiations that reach the cells, which results in a lower rate of inactivation.

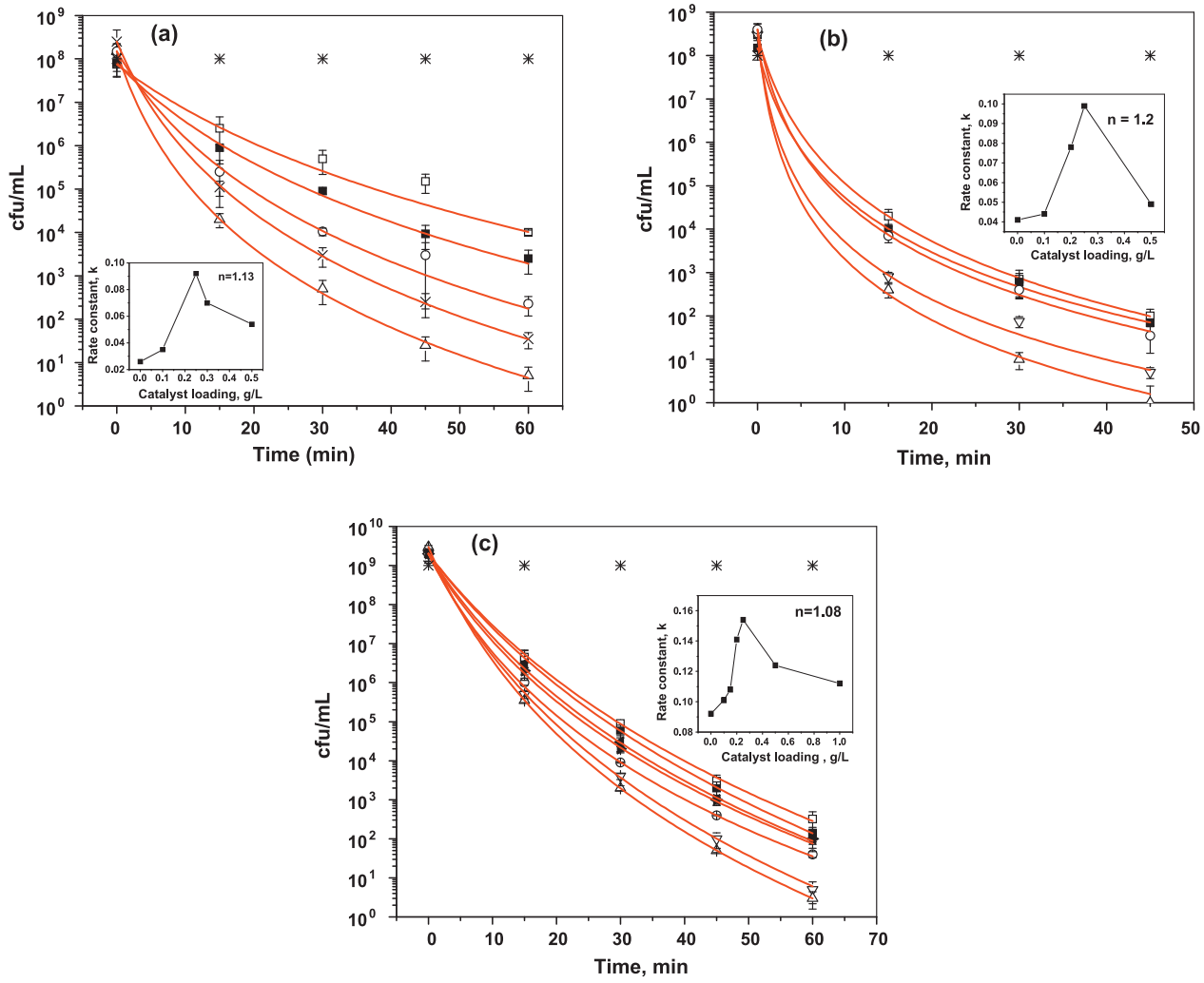

Fig. 1. Effect of CS–TiO_2 catalyst loading on inactivation of (a) ~10^8 cfu/mL *E. coli* with lamp intensity 2 W/m^2, (b) ~10^8 cfu/mL *E. coli* with lamp intensity 64 W/m^2 and (c) ~10^8 cfu/mL *P. pastoris* with lamp intensity 64 W/m^2. Lines indicate model fit. Inset shows the variation of rate constant, *k*, with the catalyst concentration. (□) photolysis; (*) dark; (■) 0.1 g/L; (◄) 0.15 g/L; (▽) 0.2 g/L; (△) 0.25 g/L; (x) 0.3 g/L; (○) 0.5 g/L; (►) 1 g/L.

The above effect was also observed with the degradation of chemical contaminants (reported as shadowing effect) [31], and few of the earlier studies (reported as screening effect) [4]. There are several reports showing different optimum catalyst concentration [4,5,32]. The optimum catalyst concentration depends on various operating parameters like photocatalytic reactor geometry, type of light source, pH, etc. Few studies also showed that at high lamp intensity, the inactivation rate increases and do not depend on catalyst concentration [5,33].

To check the effect of light intensity on the inactivation of *E. coli*, the above experiments with varying catalyst loading were conducted at a light intensity of 64 W/m^2 (Fig. 1(b)). At this intensity, photolysis alone was observed to have a significant effect on inactivation and a total reduction of 6-log in the plate count was observed within 45 min of irradiation time. The optimum catalyst loading was 0.25 g/L and complete inactivation of *E. coli* was observed within 45 min. This shows that with increase in lamp intensity, the inactivation time reduced but the optimum catalyst concentration was unchanged.

There are two major stages in the inactivation of *E. coli*: fast inactivation within first 15 min followed by a slower inactivation during 15–45 min. Some studies [4,20] have reported a three step inactivation process, which includes an additional initial induction period of 5 min, in which *E. coli* resists the effect of ROS by a self-defense mechanism. During the fast inactivation period, very high concentration of ROS causes damage to the outer cell wall and the membrane components of the bacteria resulting in the inactivation of the cell [4,24]. In the final step, due to presence of inactivated cells and cells components, ROS has only a small effect on the live cells and therefore a slow inactivation was observed [4,24].

Several studies have reported the photocatalytic inactivation of microorganisms to follow first-order reaction kinetics [6,20,34]. Few reports [22] used two exponential decay equation and calculated rate constants in slow and fast inactivation steps separately.

A power law based kinetics can be used to determine the inactivation rates. The rate expression of the form $r = kC^n$, where *r* is rate of inactivation, *k* is reaction rate constant (cfu/mL)$^{(1-n)}$/min, *C* is plate count (cfu/mL) and *n* is the order of reaction can be solved to yield:

$$\mathrm{Log}\left(\frac{C}{C_0}\right) = \frac{\mathrm{Log}\{1 + [(n-1)ktC_0^{(n-1)}]\}}{1-n} \quad (1)$$

The values of rate constant (*k*) and order of reaction (*n*) are calculated for each inactivation pattern for *E. coli* in Fig. 1(a) and (b) using non-linear regression analysis (using Origin software) and the results are shown in Tables SI 1 and SI 2 (see supplementary information), respectively. Initially both *k* and *n* were set as variables but it was observed that the value of n was close to 1.13 for all inacti-

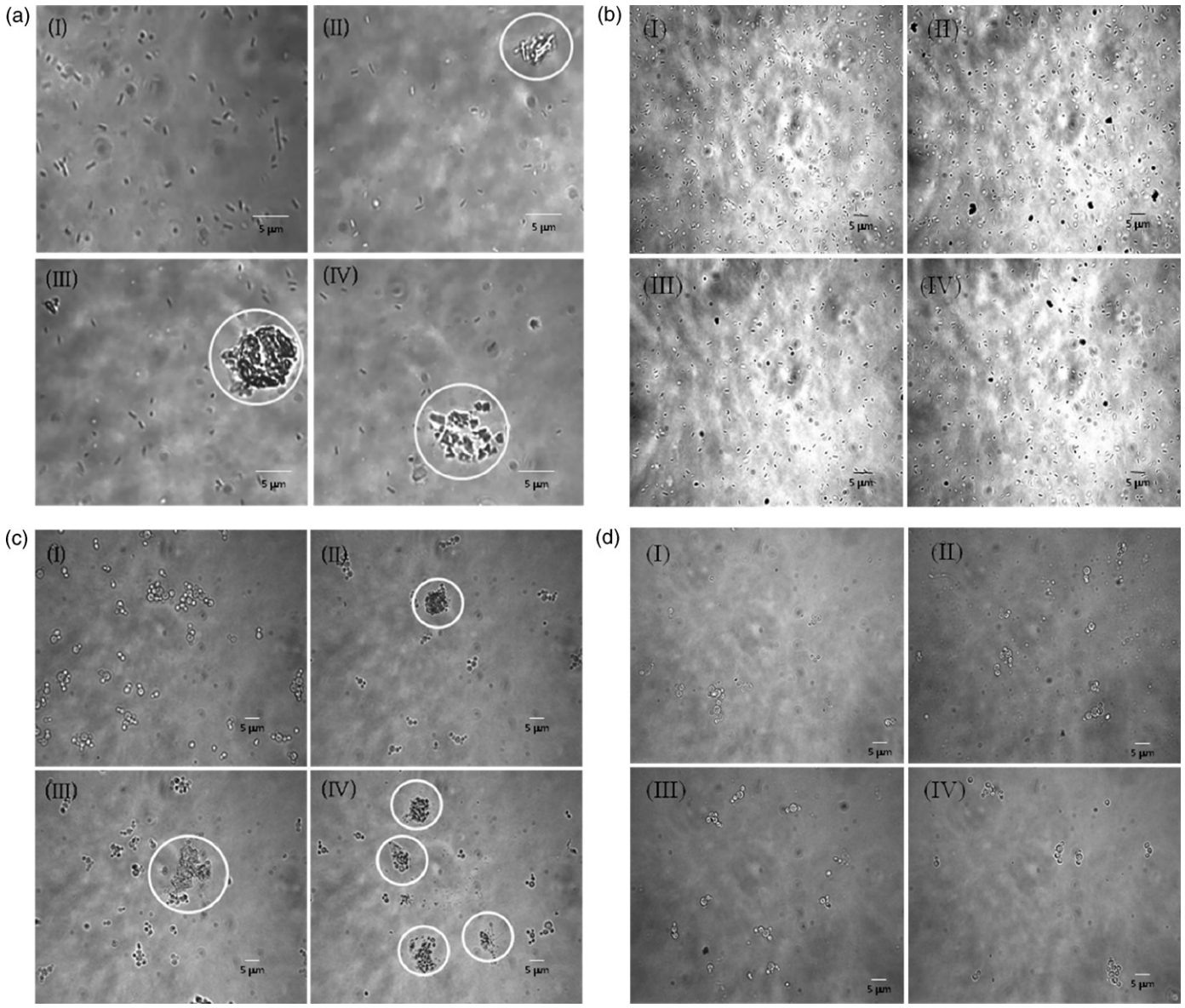

Fig. 2. Inverted microscope images of (a) inactivation of *E. coli* with 0.25 g/L CS–TiO_2, lamp intensity 64 W/m^2: (I) 0 min, (II) 15 min, (III) 30 min and (IV) 45 min; (b) inactivation of *E. coli* with 0.25 g/L CS–TiO_2, dark experiment: (I) 0 min, (II) 15 min, (III) 30 min and (IV) 45 min; (c) inactivation of *P. pastoris* with 0.25 g/L CS–TiO_2, lamp intensity 64 W/m^2: (I) 0 min, (II) 15 min, (III) 45 min and (IV) 60 min. (d) Inactivation of *P. pastoris* with 0.25 g/L CS–TiO_2, dark experiment: (I) 0 min, (II) 15 min, (III) 45 min and (IV) 60 min. The encircled portions are the observed cell bunches.

vation patterns in Fig. 1(a) and 1.2 for all the inactivation patterns in Fig. 1(b). Therefore, the order of reaction, *n*, was fixed at 1.13 and 1.2 for lamp intensity 2 W/m^2 and 64 W/m^2, respectively. At this order of reaction, the values of rate constants were calculated. As observed experimentally, the value of k increases with catalyst loading up to the catalyst concentration of 0.25 g/L. The values of rate constants decreased with the further increase in catalyst loading, as observed experimentally. Insets in Fig. 1(a) and (b) shows the variation of rate constant, *k*, with the catalyst concentration.

Fig. 2(a) shows the inverted microscope images of *E. coli* during the course of reaction. The experiment was carried out with 0.25 g/L CS–TiO_2 catalyst and with a lamp intensity of 64 W/m^2. The cells were undiluted and were taken on a sterile glass slide for microscopy. The first image (Fig. 2(a) (I)) is at the beginning of experiment, where all the cells were healthy. After 15 min (Fig. 2(a) (II)), bunch of cells were observed (encircled), which could be inactivated cells. Thus we hypothesize that after the first step of fast inactivation, the dead or inactivated cells along with cell components would have covered the live cells and thus protected them from further damage. Therefore, slow inactivation was observed after 15 min. As irradiation time increased, cell bunches were observed to be of larger size (encircled portion in Fig. 2(a) (III)). Further irradiation resulted in the damage of these bunches (Fig. 2(a) (IV)), which is at the end of 45 min of irradiation. The results obtained were compared with the dark experiment (Fig. 2(b)). It was observed that observed cell bunches were very small and does not grow in sizes, unlike photocatalysis experiments. Though the inverted microscopy gives a brief overview of morphology, it is not possible to study the changes on the cell wall with inverted microscopy. Therefore, SEM was used to obtain a closer view of the cell wall. Fig. 3(a) (I) shows the SEM image of healthy *E. coli* cells in the beginning of experiment. Fig. 3(a) (II) shows the image after 15 min irradiation, in which some of the cells were observed to be dead and broken at many places (inset in Fig. 3(a) (II)). The wrapping of dead cell material around single *E. coli* cell after 45 min irradiation was observed (Fig. 3(a) (III)). Various studies have reported simi-

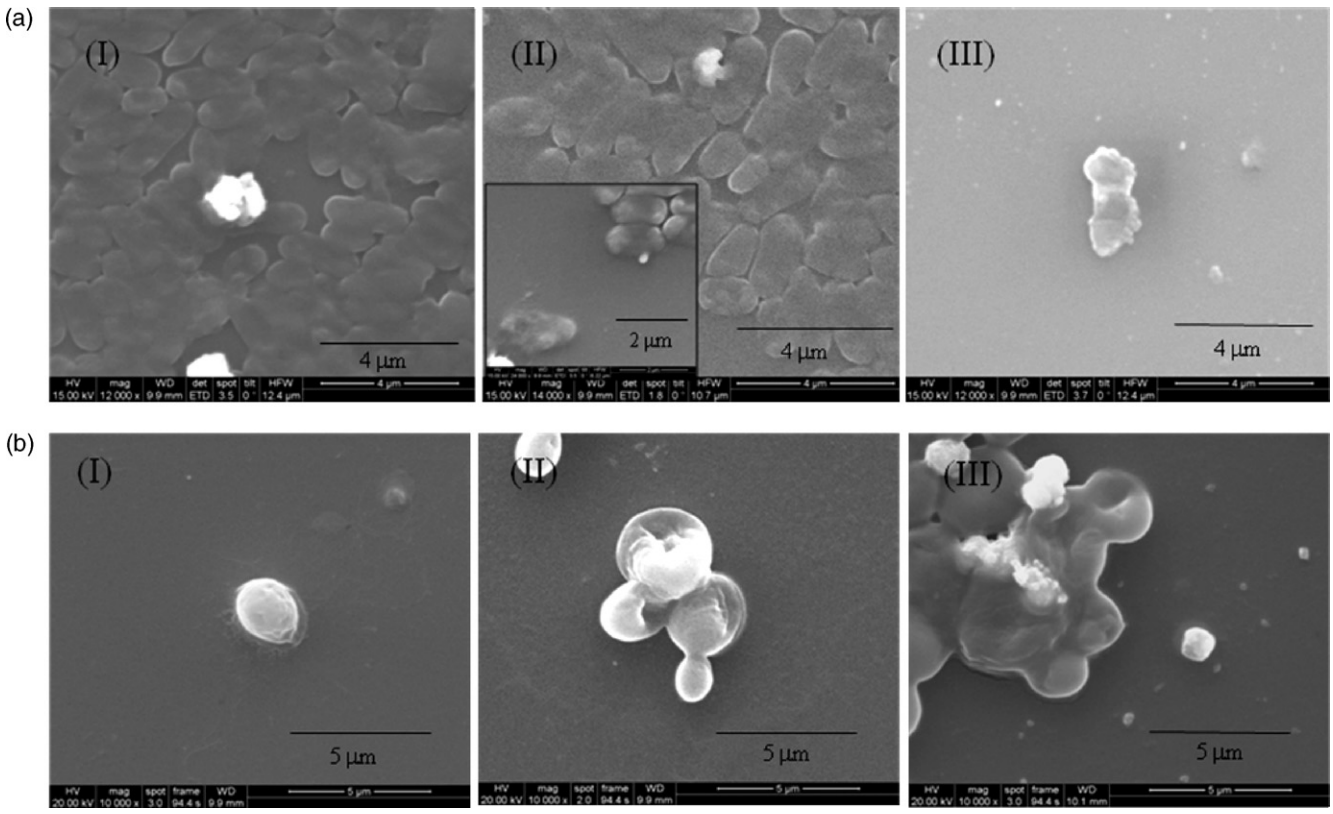

Fig. 3. SEM images of (a) *E. coli* and (b) *P. pastoris*, at (I) 0 min, (II) 15 min and (III) 45 min.

lar type of observations when inactivated microorganisms were analyzed with SEM images [35,36].

The effect of catalyst concentration was also studied for the inactivation of *P. pastoris* and the results are shown in Fig. 1(c). The experiments were done with a lamp intensity of 64 W/m^2. The initial cell concentration of *P. pastoris* was $\sim 10^9$ cfu/mL. Photolysis alone had less effect on inactivation compared to that observed with *E. coli*. There was no reduction in the plate count for the dark experiment. Similar to *E. coli*, when catalyst loading was increased from 0.1 g/L to 0.25 g/L, the rate of inactivation increased. At 0.25 g/L, maximum inactivation was observed and any further increase in catalyst loading resulted in decreased rate of inactivation. This shows that 0.25 g/L as the optimum catalyst loading for the inactivation of *P. pastoris* also. Two steps of inactivation were observed also in this case. The cells were irradiated for 60 min, with the optimum catalyst loading of CS-TiO_2. After 60 min, complete inactivation was observed. The inactivation patterns were modeled using Eq. (1) and the results are shown in Table SI 3. *P. pastoris* was observed to follow an order of reaction of 1.08. At optimum catalyst loading of 0.25 g/L, the inactivation rate constant, *k*, was 0.154 $(\text{cfu/mL})^{(1-n)}$/min. During the course of reaction, the cell morphology was studied using inverted microscope and SEM. Fig. 2(c) shows the inverted microscope images of *P. pastoris*. Cells were observed to form bunches with an increase in irradiation time, as shown in Fig. 2(c) (II) and Fig. 2(c) (III). At the end of 60 min, damage to the bunches was observed (Fig. 2(c) (IV)), similar to that observed in case of *E. coli*. In this case also dark experiments were observed to have no cell bunches formation (Fig. 2(d)). The SEM images of *P. pastoris* at different stages of inactivation are shown in Fig. 3(b). Similar results were also observed in case of *P. pastoris*. This supports the hypothesis of possibility of wrapping of cell with dead cell material. From the images, we can hypothesize that cell wall rupture was probably the main cause of cell inactivation.

It was observed that when the cells were exposed to the same light intensity, *E. coli* and *P. Pastoris* followed two different kinetics of inactivation. The order of reaction, *n*, was 1.2 in case of *E. coli* whereas it was 1.08 for *P. pastoris*. *E. coli* is a Gram (−) bacteria, whereas *P. pastoris* is a yeast. The difference in the inactivation order could be attributed to the different cell structures, particularly cell wall, of the two microorganisms. The cell wall of Gram (−) bacteria is thinner and weaker than yeast and Gram (+) bacteria. The thin cell wall cannot protect the Gram (−) bacteria from reactive oxygen species [20] and thus photolysis alone can damage the cells to a major extent. However, the presence of β-D-glucans and chitins are responsible for the higher strength of yeast cell wall [20] and thus are more resistant to photolysis.

3.2.2. Effect of different catalysts

At an optimum concentration of 0.25 g/L, the microorganism-catalyst suspensions were irradiated using four different catalysts. It was observed that the optimum loading remains the same i.e. 0.25 g/L for DP-25 and Ag doped TiO_2 catalysts (not included here), therefore the comparison has been done. The results are shown in Fig. 4(a) and (b) (*E. coli*) and (c) (*P. pastoris*). The inset in the figures shows the graph of catalyst versus rate constant, *k*. The inactivation of both microorganisms in presence of all combustion synthesized catalysts was higher than that observed with commercial Degussa catalyst (DP-25). Among all catalysts used, Ag/TiO_2 (Imp) exhibited the maximum inactivation potential for the inactivation of both the microorganisms. Ag/TiO_2 (Sub) showed lower photocatalytic activity than other combustion synthesized catalysts but more than DP-25. Thus the order of activity is Ag/TiO_2 (Imp) > CS–TiO_2 > Ag/TiO_2 (Sub) > DP-25. This can be attributed to the intensity of the fluorescence spectra (Fig. SI 7 (see supplementary information)). The emission at 425 nm of 2.9 eV can be attributed to the free excitation, and the emission at 489 nm corresponding to 2.53 eV, can be due to the transition from defect sites

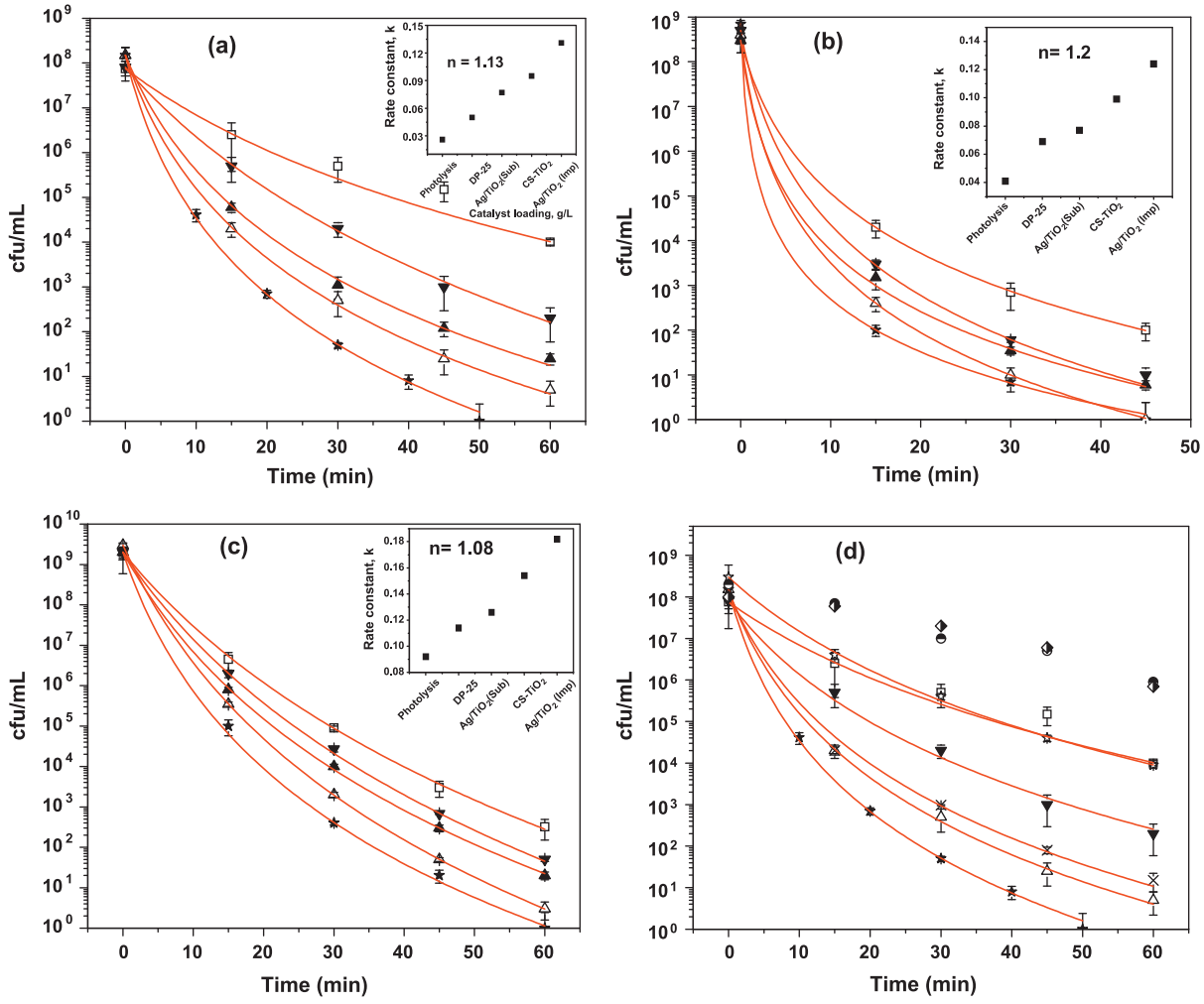

Fig. 4. Effect of different catalysts on inactivation of (a) *E. coli* with lamp intensity 2 W/m^2, (b) *E. coli* with lamp intensity 64 W/m^2, (c) *P. pastoris* with lamp intensity 64 W/m^2 and (d) *E. coli* with lamp intensity 2 W/m^2; a comparison between bare and silver impregnated catalysts. Lines indicate model fit. Inset shows the variation of rate constant, *k*, with different catalyst. (□) photolysis; (▼) DP-25, (▲) Ag/TiO_2 (Sub); (△) CS-TiO_2; (*) Ag/TiO_2 (Imp); (☆) Al_2O_3; (x) Ag/Al_2O_3 (Imp); (3) Ag/TiO_2 (Imp), dark; (T) Ag/Al_2O_3 (Imp), dark.

like oxygen vacancy to the Ti(3d) state [17]. This can be ascribed to the non-radiative recombination of charge carriers, which are trapped in the Ag(3d) energy level below the conduction band in the case of Ag/TiO_2 (Sub), and in the Schottky barrier formed in the Ag–TiO_2 interface in the case of Ag/TiO_2 (Imp) [17,37]. It is well reported that the substitution of metal ions into the TiO_2 lattice results in the generation of oxide ion vacancy. Hence, in case of Ag/TiO_2 (Sub), these vacancies can act like trapping sites for electrons [17]. Thus Ag/TiO_2 (Imp) may provide more inactivation efficiency than other three catalysts. The presence of silver on the catalyst surface plays an important role in charge separation upon light absorption and improves photochemical activity of TiO_2 based catalysts [22]. The increase in the rate of reaction and decrease in extent of reaction time for *E. coli* inactivation was observed by increasing the lamp intensity with all combustion synthesized and commercial catalyst.

To check the effect of silver on inactivation of *E. coli*, Ag was impregnated on Al_2O_3 and the results are shown in Fig. 4(d). The inactivation in the presence or absence (photolysis) of Al_2O_3 catalyst alone was almost identical. In other words, Al_2O_3 alone did not display any photocatalytic activity. However, when Ag/Al_2O_3(Imp) was used, the inactivation rate increased and 7-log reduction in the plate count was observed within 60 min. Thus the enhanced reduction (approximately 3-log) in the plate count can be attributed to the presence of impregnated silver. The results were also compared with the dark experiments with Ag/TiO_2 (Imp) and Ag/Al_2O_3 (Imp) (Fig. 4(d)). Both experiments show reduction of 3-log in the plate count, which can be due to the presence of silver alone. Silver has antimicrobial properties and it also helps in enhancing the surface adhesion properties of the system, which is an important step of the inactivation reaction [22]. Therefore, when it is impregnated on a non-photocatalytic catalyst like alumina, it shows significant activity. The result shows that rate of inactivation can be enhanced by impregnating the catalysts with silver ions.

The values of rate constant and order of reaction for each inactivation pattern in Fig. 4(a), (b), (c) and (d) were calculated using Eq. (1) and the values are shown in Tables SI 4, SI 5, SI 6 and SI 7 (see supplementary information), respectively. It is observed that order of reaction, *n*, using different catalysts remained the same for both the microorganisms.

3.2.3. *Effect of different initial cell concentration*

Fig. 5(a) and (b) shows the effect different initial cell concentrations of E. coli at an optimum catalyst loading of Ag/TiO2 (Imp), with a lamp intensity of 2 W/m2 and 64 W/m2, respectively. Benabbou et al. [4] reported that catalyst loading and initial concentration of E. coli are independent and therefore optimum catalysts loading are independent of the initial concentration. Fig. 5(c) shows the

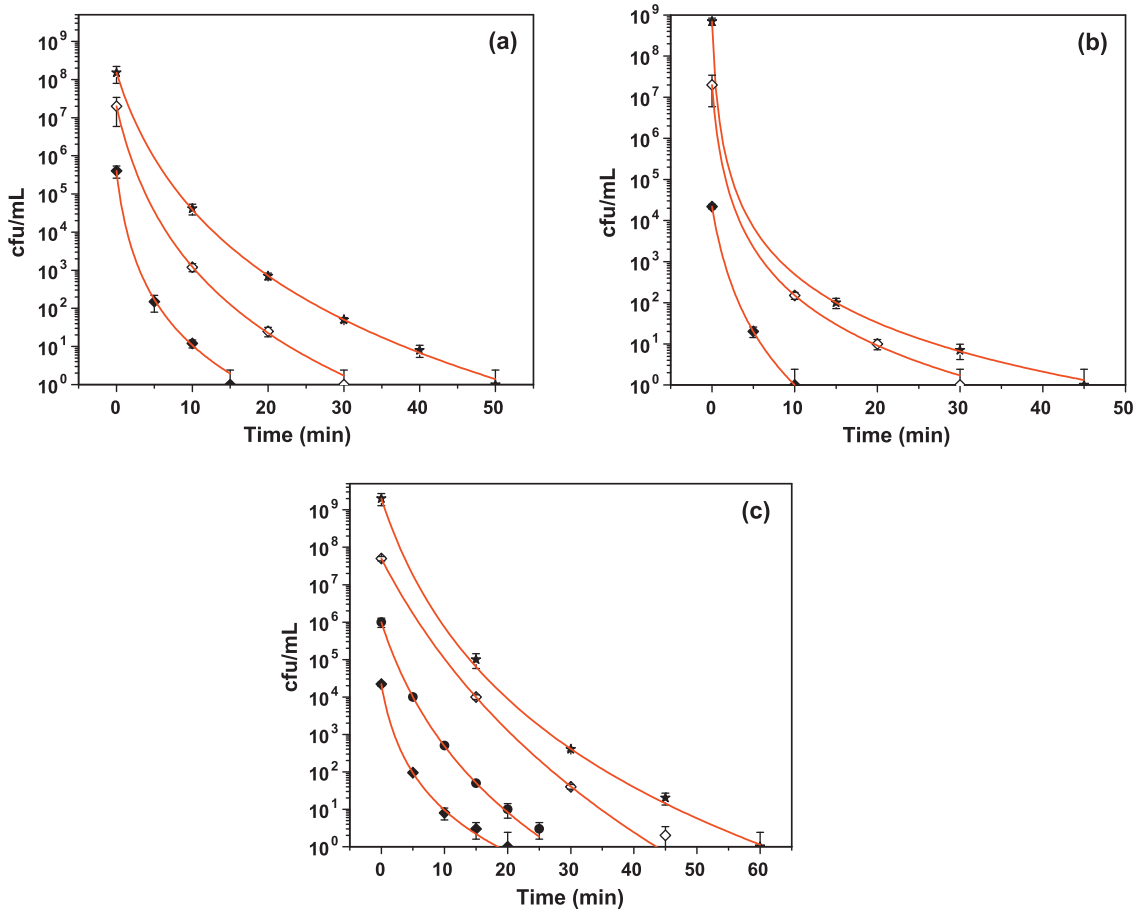

Fig. 5. Effect of different initial cell concentrations on inactivation of (a) *E. coli* with lamp intensity 2 W/m^2, (b) *E. coli* with lamp intensity 64 W/m^2, (c) *P. pastoris* with lamp intensity 64 W/m^2. Catalyst loading: 0.25 g/L. (*) 10^8 cfu/mL; (◊) 10^7 cfu/mL; (●) 10^6 cfu/mL; (♦) 10^5 cfu/mL.

effect different initial cell concentrations of P. pastoris at an optimum catalyst loading of Ag/TiO2 (Imp), with a lamp intensity of 64 W/m2. It was observed for E. coli, when the cell concentration ranged from 108 to 109 cfu/mL, there was complete inactivation, within 45–50 min of irradiation. However, for P. pastoris, when initial cell concentration ranged 109–1010, complete inactivation was observed with 60 min of irradiation time. Decreasing the initial cell concentration of both the microorganisms to 107–108 cfu/mL, increased the rate of inactivation. Total inactivation of E. coli cells were observed within 30 min while complete inactivation of P. pastoris was observed within 45 min of irradiation. At a low concentration of 104–105 cfu/mL, the inactivation process became fast and 10–15 min was sufficient to kill the total amount of bacteria while it took 20 min for complete inactivation of P. pastoris. This shows that at lower initial cell concentration and at optimum catalyst loading, rapid and complete inactivation of E. coli is possible compared to P. pastoris. As discussed earlier, the difference in the cell wall structure could be the possible reason for different inactivation mechanisms.

4. Conclusions

The results demonstrate the potential of microorganism inactivation using UV irradiation in presence of combustion synthesized catalysts. The photocatalytic activity of all combustion synthesized catalysts was higher than that observed with was more than commercial Degussa catalyst. The optimum catalyst concentration was 0.25 g/L and the maximum inactivation of both microorganisms was observed in the presence of 1% Ag impregnated TiO_2. The reasons for the higher activity of Ag/TiO_2 (Imp) TiO_2 were provided. Rapid and complete inactivation of both the microorganisms was observed at lower initial cell concentrations. *E. coli* and *P. pastoris* followed different kinetics of inactivation and the rate constants and the order of the reaction were determined. Images obtained from inverted microscope and SEM suggest cell wall rupture as the main cause of inactivation.

Acknowledgement

Financial support from the Department of Science and Technology, Government of India is gratefully acknowledged.

Appendix A. Supplementary data

Supplementary data associated with this article can be found, in the online version, at doi:10.1016/j.cej.2010.09.021.

References

[1] T. Matsunaga, R. Tomada, T. Nakajima, H. Wake, Photoelectrochemical sterilization of microbial cells by semiconductor powders, FEMS Microbiol. Lett. 29 (1985) 211–214.
[2] D.M. Blake, P.-C. Maness, Z. Huang, E.J. Wolfrum, J. Huang, W.A. Jacoby, Application of the photocatalytic chemistry of titanium dioxide to disinfection and the killing of cancer cells, Sep. Purif. Methods 28 (1999) 1–50.
[3] Y. Horie, D.A. David, M. Taya, S. Tone, Effects of light intensity and titanium dioxide concentration on photocatalytic sterilization rates of microbial cells, Ind. Eng. Chem. Res. 35 (1996) 3920–3926.
[4] A.K. Benabbou, Z. Derriche, C. Felix, P. Lejeune, C. Guillard, Photocatalytic inactivation of *Escherichia coli*—effect of concentration of TiO_2 and microorganism, nature, and intensity of UV irradiation, Appl. Catal. B: Environ. 76 (2007) 257–263.

[5] A.G. Rincón, C. Pulgarin, Photocatalytical inactivation of *E. coli*: effect of (continuous-intermittent) light intensity and of (suspended–fixed) TiO_2 concentration, Appl. Catal. B: Environ. 44 (2003) 263–284.
[6] A.G. Rincón, C. Pulgarin, Bactericidal action of illuminated TiO_2 on pure *Escherichia coli* and natural bacterial consortia: post-irradiation events in the dark and assessment of the effective disinfection time, Appl. Catal. B: Environ. 49 (2004) 99–112.
[7] A.G. Rincón, C. Pulgarin, Effect of pH, inorganic ions, organic matter and H_2O_2 on E. coli K12 photocatalytic inactivation by TiO_2: implications in solar water disinfection, Appl. Catal. B: Environ. 51 (2004) 263–302.
[8] P.-C. Maness, S. Smolinski, D.M. Blake, Z. Huang, E.J. Wolfrum, W.A. Jacoby, Bactericidal activity of photocatalytic TiO_2 reaction, Appl. Environ. Microbiol. 65 (1999) 4094–4098.
[9] K. Sunada, T. Watanabe, K. Hashimoto, Bactericidal activity of copper-deposited TiO_2 thin film under weak UV light illumination, Environ. Sci. Technol. 37 (2003) 4785–4789.
[10] K. Tanaka, M.F.V. Capule, T. Hisanaga, Effect of crystallinity of TiO_2 on its photocatalytic action, Chem. Phys. Lett. 187 (1991) 73–76.
[11] M.R. Hoffmann, S.T. Martin, W. Choi, D.W. Bahnemann, Environmental applications of semiconductor photocatalysis, Chem. Rev. 95 (1995) 69–96.
[12] A. Linsebigler, G. Lu, J.T. Yates, Photocatalysis on TiO_2 surfaces: principles, mechanisms, and selected results, Chem. Rev. 95 (1995) 735–758.
[13] L.K. Campbell, B.K. Na, E.I. Ko, Synthesis and characterization of titania aerogels, Chem. Mater. 4 (1992) 1329–1333.
[14] E. Stathatos, P. Lianos, F. DelMonte, D. Levi, D. Tsiourvas, Formation of TiO_2 nanoparticles in reverse micelles and their deposition as thin films on glass substrates, Langmuir 13 (1997) 4295–4300.
[15] C.D. Terwilliger, Y.-M. Chiang, Characterization of chemically and physically derived nanophase titanium dioxide, Nanostruct. Mater. 2 (1993) 37–45.
[16] M.S. Hegde, G. Madras, K.C. Patil, Noble metal ionic catalysts, Acc. Chem. Res. 42 (2009) 704–712.
[17] K. Nagaveni, M.S. Hegde, G. Madras, Structure, photocatalytic activity of $Ti_{1-x}M_xO_{2\pm\delta}$ (M = W, V, Ce, Zr, Fe, and Cu) synthesized by solution combustion method, J. Phys. Chem. B 108 (2004) 20204–20212.
[18] K. Nagaveni, G. Sivalingam, M.S. Hegde, G. Madras, Photocatalytic degradation of organic compounds over combustion-synthesized nano-TiO_2, Environ. Sci. Technol. 38 (2004) 1600–1604.
[19] Sivalingam, K. Nagaveni, M.S. Hegde, G. Madras, Photocatalytic degradation of various dyes by combustion synthesized nano anatase TiO_2, Appl. Catal. B: Environ. 45 (2003) 23–38.
[20] A. Erkan, U. Bakir, G. Karakas, Photocatalytic microbial inactivation over Pd doped SnO_2 and TiO_2 thin films, J. Photochem. Photobiol. A 184 (2006) 313–321.
[21] C. Hu, J. Guo, J. Qu, X. Hu, Photocatalytic degradation of pathogenic bacteria with AgI/TiO_2 under visible light irradiation, Langmuir 23 (2007) 4982–4987.
[22] A. Kubacka, M. Ferrer, A. Martínez-Arias, M. Fernández-García, Ag promotion of TiO_2-anatase disinfection capability: study of *Escherichia coli* inactivation, Appl. Catal. B: Environ. 84 (2008) 87–93.
[23] M.T. Hedayeti, A.C. Pasqualotto, P.A. Warn, P. Bowyer, D.W. Denning, *Aspergillus flavus*: human pathogen, allergen and mycotoxin producer, Microbiology 153 (2007) 1677–1692.
[24] D Mitoraj, A. Jańczyk, M. Strus, H. Kisch, G. Stochel, P.B. Heczko, W. Macyk, Visible light inactivation of bacteria and fungi by modified titanium dioxide, Photochem. Photobiol. Sci. 6 (2007) 642–648.
[25] C. Sichel, M. de Cara, J. Tello, J. Blanco, P. Fernández-Ibáñez, Effect of UV solar intensity and dose on the photocatalytic disinfection of bacteria and fungi, Appl. Catal. B: Environ. 74 (2007) 152–160.
[26] O. Seven, B. Dindar, S. Aydemir, D. Metin, M.A. Ozinel, S. Icli, Solar photocatalytic disinfection of a group of bacteria and fungi aqueous suspensions with TiO_2, ZnO and Sahara desert dust, J. Photochem. Photobiol. A 165 (2004) 103–107.
[27] H. Le Pape, F. Solano-Serena, P. Contini, C. Devillers, A. Maftah, P. Leprat, Evaluation of the anti-microbial properties of an activated carbon fibre supporting silver using a dynamic method, Carbon 40 (2002) 2947–2954.
[28] R. Fischer, J. Drossard, N. Emans, U. Commandeur, S. Hellwig, Towards molecular farming in the future: *Pichia pastoris*-based production of single-chain antibody fragments, Biotechnol. Appl. Biochem. 30 (1999) 117–120.
[29] R. Vinu, G. Madras, Photocatalytic activity of Ag-substituted and impregnated nano-TiO_2, Appl. Catal. A 366 (2009) 130–140.
[30] K.L. Willett, R.A. Hites, Chemical, actinometry: using o-nitrobenzaldehyde to measure light intensity in photochemical experiments, J. Chem. Educ. 77 (2000) 900–902.
[31] K. Nagaveni, G. Sivalingam, M.S. Hegde, G. Madras, Solar photocatalytic degradation of dyes: high activity of combustion synthesized nano TiO_2, Appl. Catal. B: Environ. 48 (2004) 83–93.
[32] H.M. Coleman, C.P. Marquis, J.A. Scott, S.-S. Chin, R. Amal, Bactericidal effects of titanium dioxide-based photocatalysts, Chem. Eng. J. 113 (2005) 55–63.
[33] F. Chen, X. Yang, Q. Wu, Photocatalytic oxidation of *Escherischia coli*, *Aspergillus niger*, and formaldehyde under different ultraviolet irradiation conditions, Environ. Sci. Technol. 43 (2009) 4606–4611.
[34] J. Ibáñez, M. Litter, R. Pizarro, Photocatalytic bactericidal effect of TiO_2 on Enterobacter cloacae: comparative study with other Gram (−) bacteria, J. Photochem. Photobiol. A 157 (2003) 81–85.
[35] K.P. Kühn, I.F. Chaberny, K. Massholder, M. Stickler, V.W. Benz, H.-G. Sonntag, L. Erdinger, Disinfection of surfaces by photocatalytic oxidation with titanium dioxide and UVA light, Chemosphere 53 (2003) 71–77.
[36] K.S. Yao, D.Y. Wang, J.J. Yan, L.Y. Yang, W.S. Chen, Photocatalytic effects of TiO_2/Fe thin film irradiated with visible light on cellular surface ultrastructure and genomic DNA of bacteria, Surf. Coat. Technol. 201 (2007) 6882–6885.
[37] X.-G. Hou, M.-D. Huang, X.-L. Wu, A.-D. Liu, Preparation and studies of photocatalytic silver-loaded TiO_2 films by hybrid sol–gel method, Chem. Eng. J. 146 (2009) 42–48.